ACS Catalysis

Research Article

pubs.acs.org/acscatalysis

Implications of CO_2 Activation by Frustrated Lewis Pairs in the Catalytic Hydroboration of CO_2: A View Using N/Si^+ Frustrated Lewis Pairs

N. von Wolff, G. Lefèvre, J.-C. Berthet, P. Thuéry, and T. Cantat*

NIMBE, CEA, CNRS, Université Paris-Saclay, Gif-sur-Yvette, France

Supporting Information

ABSTRACT: A series of base-stabilized silylium species were synthesized and their reactivity toward CO_2 explored, yielding the characterization of a novel N/Si^+ FLP-CO_2 adduct. These silicon species are active catalysts in the hydroboration of CO_2 to the methoxide level with 9-BBN, catecholborane (catBH), and pinacolborane (pinBH). Both experiments and DFT calculations highlight the role of the FLP-CO_2 adduct in the catalysis. Depending on the nature of the hydroborane reductant, two distinct mechanisms have been unveiled. While 9-BBN and catBH are able to reduce an intermediate FLP-CO_2 adduct, the hydroboration of CO_2 with pinBH follows a different and novel path where the B−H bond is activated by the silicon-based Lewis acid catalyst. In these mechanisms, the formation of a highly stabilized FLP-CO_2 adduct is found detrimental to the kinetics of the reaction.

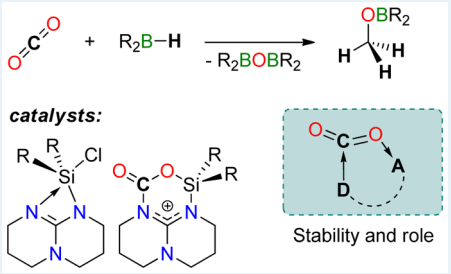

KEYWORDS: *organocatalysis, CO_2, hydroboration, mechanisms, DFT calculations*

INTRODUCTION

Carbon dioxide is an abundant, inexpensive, low toxic, and renewable carbon feedstock and therefore an appealing C1-building block in organic chemistry.[1−3] The efficient reduction of CO_2 to important raw materials for the chemical industry or to value-added chemicals is, however, hampered by its high thermodynamic stability and kinetic inertness toward reduction. This drawback calls for efficient reduction catalysts able to synchronize C−O bond cleavage with C−H and C−C bond formation, at a high kinetic rate and with a low energy demand. While CO_2 activation and reduction at a metal center has been thoroughly investigated over the last four decades,[2,4−8] organic systems able to perform this task, based on main group elements (e.g., B, N, O, P, and Si), remain sporadic and underexplored. Many different coordination modes have been unveiled for the interaction of CO_2 with a transition metal or an f-element, based on the nature of the metal ion and the redox state of the CO_2 ligand.[9,10] In organic chemistry, CO_2 activation is quite monotonous and relies on the formation of stable adducts with organic Lewis bases, such as guanidines or N-heterocyclic carbenes (NHCs).[11−13] Nevertheless, most progress has been gained via the synergistic action of Lewis pairs, able to coordinate both the C and O centers of CO_2. Within the concept of frustrated Lewis pairs (FLPs), introduced by Stephan and Erker,[14−17] several CO_2 adducts have been successfully isolated over the last 6 years, in which the C atom is attached to a C, N, or P donor, while one or two O atoms coordinate a group XIII Lewis acid (B or Al).[18−28] Although FLP-CO_2 adducts are commonly proposed as catalytic intermediates in the reduction of CO_2 with hydrosilanes or hydroboranes, their possible involvement and role in the catalysis remain yet unclear.[29−34] Experimentally, FLPs that catalyze the hydroelementation of CO_2 do not form observable adducts with CO_2, and conversely, only a single N/B FLP-CO_2 adduct has been reported so far to promote the catalytic hydroboration of CO_2 by our group.[27,35] Mechanistically, CO_2 adducts may have a decreased reactivity compared to that of free CO_2 in the presence of a reductant, and reactive CO_2 adducts that are not thermodynamically favored under catalytic conditions may form without being detected.

In order to better address the role and influence of CO_2 adducts in the metal-free catalytic reduction of CO_2, we have thus sought stable CO_2 adducts able to perform as catalysts in the hydroboration of CO_2. Whereas FLP-CO_2 adducts mostly feature borane or alane Lewis acids, we reasoned that an isolobal and isoelectronic silylium cation (R_3Si^+) would exhibit a stronger Lewis acidity and a greater affinity for the O-center in CO_2. In addition, the versatile synthesis of organosilicon compounds may facilitate the access to structures exhibiting different affinities for CO_2. In fact, a few FLP systems involving highly electrophilic silyl cations in combination with phosphines as Lewis base were reported to activate small molecules. In 2011, Müller and co-workers demonstrated that triarylsilylium cations in combination with bulky phosphines could activate H_2, and the same system was shown recently to activate CO_2 in the formation of an adduct (**I**) with the intermolecular P/Si^+ FLP (Scheme 1).[36,37] Recently, Stephan and co-workers characterized P/Si^+ FLP-CO_2 adducts (**II**)

Received: February 12, 2016
Revised: April 13, 2016

DOI: 10.1021/acscatal.6b00421
ACS Catal. 2016, 6, 4526−4535

Scheme 1. Silylium-Based FLP Systems for the Activation of Small Molecules (CO_2 and H_2)

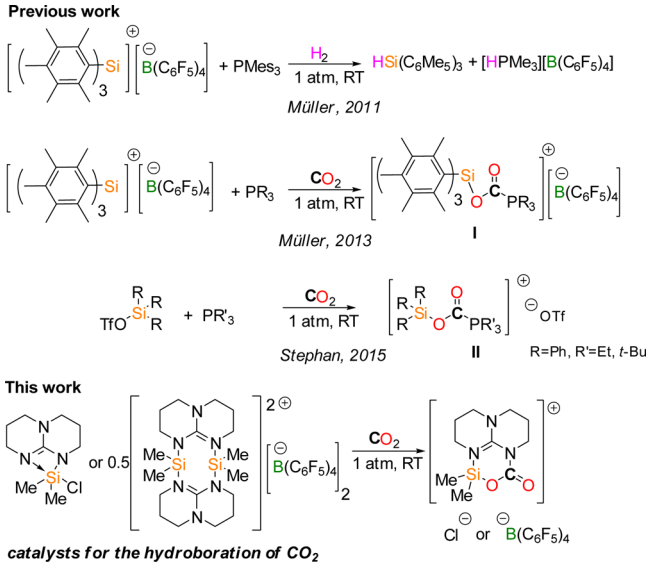

starting from basic phosphines (namely, PEt_3 and P*t*-Bu_3) and silyl triflates.[38] Further, Ashley et al. reported on a phosphine stabilized silylium species able to cleave H_2.[39] We report herein the formation of novel intramolecular FLP-CO_2 adducts by reaction of CO_2 with nitrogen stabilized silyl cations. These systems exhibit excellent catalytic activity in the hydroboration of CO_2, and the catalytic involvement of FLP-CO_2 adducts is addressed, based on mechanistic experimental, and DFT investigations (Scheme 1).

RESULTS AND DISCUSSION

Synthesis of Novel FLP-CO_2 Adducts. We recently reported that both 1,5,7-triazabicyclo[4.4.0]dec-5-ene (TBD) and guanidine substituted borane **III** are able to bind CO_2 to afford adducts **IV** and **V**, respectively (Scheme 2).[27]

Scheme 2. TBD and TBD-Substituted Borane II Form CO_2-Adducts III and IV

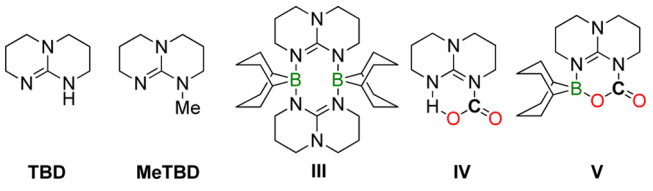

Importantly, these species are highly active hydroboration catalysts, and they promote the reduction of CO_2 to the methanol level with 9-borabicyclo[3.3.1]nonane 9-BBN, at room temperature. In order to increase the activation of the C–O bond in CO_2, the replacement of the organoborane Lewis acid with a more oxophilic silyl cation was envisioned. Unstabilized silyl cations are strong σ and π acceptors[40] and can undergo unwanted side reactions with the solvent.[41,42]

The formation of base stabilized silyl species with modulated reactivity was thus attempted by reacting the guanidinate [K^+,TBD^-] with various dichlorosilanes (Scheme 3a).

Following the procedure developed by Andell and co-workers,[43] the hypervalent chlorosilane **1** was isolated from [K^+,TBD^-] and Me_2SiCl_2. Replacing Me_2SiCl_2 with *i*-Pr_2SiCl_2 and Ph_2SiCl_2 led to the isolation of the analogous compounds ^{iPr}**1** and ^{Ph}**1**, respectively. Crystals of **1**, grown from a pentane solution, revealed a monomeric structure with a hypervalent silicon center bound to two methyl groups, the two nitrogen donors of TBD, and one chloride (Figure 1).[44] The silicon center adopts a distorted trigonal bipyramidal geometry, the Cl1 and N2 atoms occupying the axial positions with a Cl–Si–N2 bond angle of 159.20(4)°. The Si–N2 bond length is

Scheme 3. Synthesis of Hypervalent Silanes and Their Reaction with CO_2

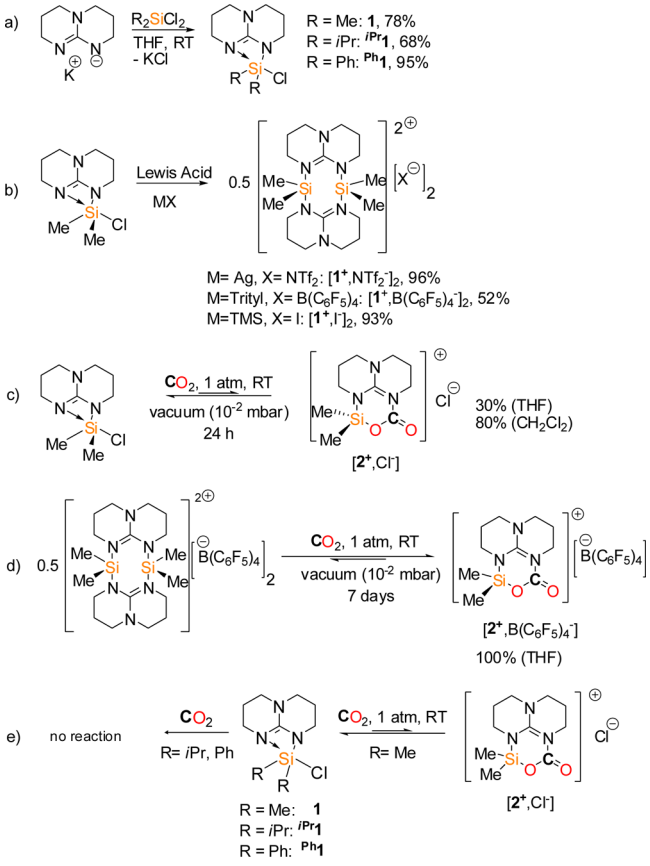

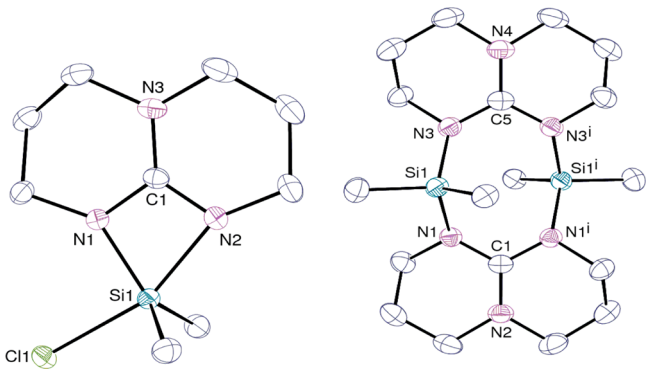

Figure 1. ORTEP view of **1** (left) and cation $(\mathbf{1}^+)_2$ in $[\mathbf{1}^+,B(C_6F_5)_4^-]_2 \cdot C_4H_8O_2$ (right). The solvent molecules and hydrogen atoms are omitted for clarity. Selected bond lengths (Å) and angles (deg) in **1**: Si1–Cl1 2.2783(5), Si1–N1 1.7914(12), Si1–N2 1.9843(12), N1–C1 1.3578(17), N2–C1 1.3087(18), and N1–Si1–N2 69.09(5). In $(\mathbf{1}^+)_2$: Si1–N1 1.7714(13), Si1–N3 1.7796(13), N1–C1 1.3628(16), and N3–C5 1.3598(17).

DOI: 10.1021/acscatal.6b00421
ACS Catal. 2016, 6, 4526–4535

significantly longer than the Si−N1 bond length (1.9843(12) vs 1.7914(12) Å), and the Si−Cl bond is elongated in comparison to Si−Cl bonds in tetravalent chlorosilanes (2.2783(5) vs, 2.01(2) Å in $SiCl_4$). Taken together, these data indicate a 3*c*/4e ω-interaction for the axial bonding.[45,46] A natural bond orbital (NBO) analysis indeed confirms a notable acidity at the Si atom with a positive charge of +1.89. A similar structure was found for ^{iPr}**1** (see SI). Treating **1** with a Lewis acid (i.e., $AgNTf_2$, $[Ph_3C][B(C_6F_5)_4]$, or Me_3SiI) readily led to the formation of dimeric dicationic species in agreement with the reported ease of halogen−silicon bond ionization of base-stabilized halosilanes (Scheme 3b).[47] Crystals suitable for X-ray analysis were obtained for both $[\mathbf{1}^+,B(C_6F_5)_4^-]_2$ and $[\mathbf{1}^+,NTf_2^-]_2$ (Figure 1 and SI). A dicationic dimeric structure is also proposed for $[\mathbf{1}^+,I^-]_2$ due to its very poor solubility in common polar solvents, such as THF, DMSO, acetonitrile, and pyridine.[48]

Having in hand a series of base-stabilized chlorosilanes and silyl cations, the activation of CO_2 was explored. Exposing a d_8-THF solution of **1** to an atmosphere of CO_2 readily produces a novel species, namely, $[\mathbf{2}^+,Cl^-]$, in 30% conversion, according to the ^{1}H and ^{13}C NMR spectra of the crude solution (see SI, Figure S22). Crystals suitable for X-ray diffraction were successfully obtained by slow diffusion of pentane into a concentrated pyridine solution of **1** under a CO_2 atmosphere. As depicted in Figure 2, $[\mathbf{2}^+,Cl^-]$ is a novel CO_2 adduct where the carbon atom coordinates to a N-donor on the TBD backbone, while one oxygen atom binds to the silylium center.

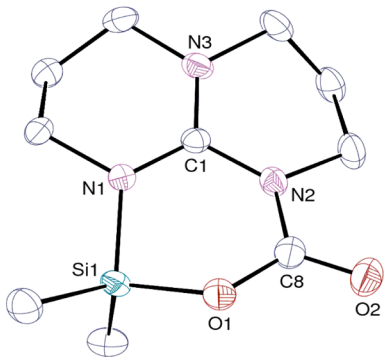

Figure 2. ORTEP view of cation $\mathbf{2}^+$ in $[\mathbf{2}^+,Cl^-]\cdot 0.5\ C_5H_5N$. The solvent molecules and hydrogen atoms are omitted for clarity. Selected bond lengths (Å) and angles (deg): Si1−O1 1.671(2), Si1−N1 1.756(2), O1−C8 1.322(4), O2−C8 1.206(4), N1−C1 1.331(4), N2−C1 1.392(4), Si1−O1−C8 125.7(2), and O1−C8−O2 121.4(3).

The formation of $\mathbf{2}^+$ also reveals that **1** can act as an intramolecular FLP. The addition of CO_2 is reversible, and **1** is recovered after evaporating a THF solution of $[\mathbf{2}^+,Cl^-]$ under high vacuum (10^{-2} mbar) overnight (Scheme 3c). Interestingly, the formation of $[\mathbf{2}^+,Cl^-]$ is more favored in CH_2Cl_2 compared to THF, and it reaches a conversion of 80% (see SI, Figure S22). This is in agreement with the observed ease of ionization of Si−Cl bonds by polar solvents reported by Kummer and co-workers,[47] and the more polar CH_2Cl_2 solvent might thus shift the equilibrium toward the ionized CO_2-adduct. Starting from $[\mathbf{1}^+,B(C_6F_5)_4^-]_2$, CO_2-adduct $[\mathbf{2}^+,B(C_6F_5)_4^-]$ is obtained quantitatively under a CO_2 atmosphere (see SI, Figure S26). This adduct shows a much greater stability as 7 days under reduced pressure (10^{-2} mbar) are needed to promote the decarboxylation of $[\mathbf{2}^+,B(C_6F_5)_4^-]$. While adducts **I** and **II**, reported by Müller et al. and Stephan et al., respectively, were found unstable and could not be characterized structurally,[38] $[\mathbf{2}^+,Cl^-]$ and $[\mathbf{2}^+,B(C_6F_5)_4^-]$ (Scheme 3d) represent the only examples of N/Si$^+$ FLP-CO_2 adducts, which are characterized structurally in the solid state. The bonding of CO_2 in adduct $\mathbf{2}^+$ resembles that of **V** and **IV**, with a more pronounced activation of the C−O bonds. Indeed, the activation of CO_2 with FLPs bends the linear CO_2 molecule, and the O−C−O bond angle is smaller in $\mathbf{2}^+$ (121.4(3) °) compared to **V** (128.6(2) °) and **IV** (129.9(2) °). In parallel, the C−O bond activated by the Lewis acid is somewhat longer in $\mathbf{2}^+$ (1.322(4) Å), compared to **V** (1.299(3) Å) and **IV** (1.257(3) Å), while the C═O bond is shorter (1.206(4) vs 1.222(2) in **V** and 1.229(2) Å in **IV**). These data confirm the stronger Lewis acidity of the silyl cation in the activation of CO_2, compared to the N/B system **V**. Spectroscopically, the ^{13}C resonance for CO_2 is shifted upfield in $\mathbf{2}^+$ (145.3 ppm, see SI Figures S25 or S23), compared to **V** and **IV** (153.1 and 154.4 ppm, respectively).

It is notable that the formation of CO_2 adducts with the intramolecular N/Si$^+$ FLPs seems sensitive to the steric crowding around the silylium center. In fact, no adduct is observed when the isopropyl or phenyl derivatives ^{iPr}**1** or ^{Ph}**1** are exposed to an atmosphere of CO_2 (Scheme 3e). This behavior provides FLP systems for which activation of CO_2 is disfavored, and hence, a platform to study the occurrence and catalytic importance of CO_2 activation by FLPs (*vide infra*).

Catalytic Hydroboration of CO_2. The catalytic hydroboration of CO_2 is an efficient method to reduce CO_2 to the methanol level under mild reaction conditions, to produce methoxyboranes or methylamines (in the presence of an amine source). This catalytic reaction, first unveiled by the Guan group in 2010 with nickel(II) catalysts,[49,50] has attracted much attention, and a variety of organometallic catalysts have been proposed.[51−53] Interestingly, in 2013, our group[27] has shown in parallel with the work of Fontaine and co-workers[31] that simple organic catalysts such as TBD, Me-TBD, or N/B, and P/B FLPs (e.g., **V**) could also serve as efficient catalysts in this reductive process. As shown with the synthesis and chemical behavior of **1**, $\mathbf{1}^+$, ^{iPr}**1**, ^{Ph}**1**, and $\mathbf{2}^+$, the introduction of a silyl cation on the guanidine backbone of TBD enables a fine-tuning in the activation of CO_2. Whereas a strong coordination of CO_2 is observed in $\mathbf{2}^+$, no reaction with CO_2 is observed in the case of ^{iPr}**1** and ^{Ph}**1** showing that the corresponding adducts are not thermodynamically favored (although they could exist as metastable intermediates). These compounds therefore constitute a suitable platform to investigate the effect of CO_2-adduct formation in the catalytic reduction of CO_2.

In the presence of 9-BBN and 1 atm of CO_2 in THF, 2.5 mol % of **1** catalyzes the hydroboration of CO_2 to the corresponding methoxyborane MeOBBN in >99% yield, after 20 h at 20 °C (Table 1, entry 1, TOF = 1.3 h^{-1}).[54] THF is the best solvent under these conditions, as both more polar (CH_3CN, pyridine) and less polar solvents (toluene, CH_2Cl_2) gave lower TOFs (Table 1, entries 2−5, TOFs up to 0.3 h^{-1}). In fact, as shown in the work of Kummer and co-workers,[47] the solvent (Gutmann donor and acceptor number) can have an important influence on the ionization of the Si−Cl bond and hence on the Lewis acidity of the silicon center. The observed solvent effects could, however, not be correlated to the respective solvent acceptor (nor donor) numbers and might therefore be due to differences in CO_2 and borane solubility. Increasing the steric bulk around silicon leads to a lower reactivity for the hydroboration of CO_2 using 9-BBN. After 24

DOI: 10.1021/acscatal.6b00421
ACS Catal. 2016, 6, 4526−4535

Table 1. Catalyst Screening for the Hydroboration of CO_2 to Methoxyboranes[a]

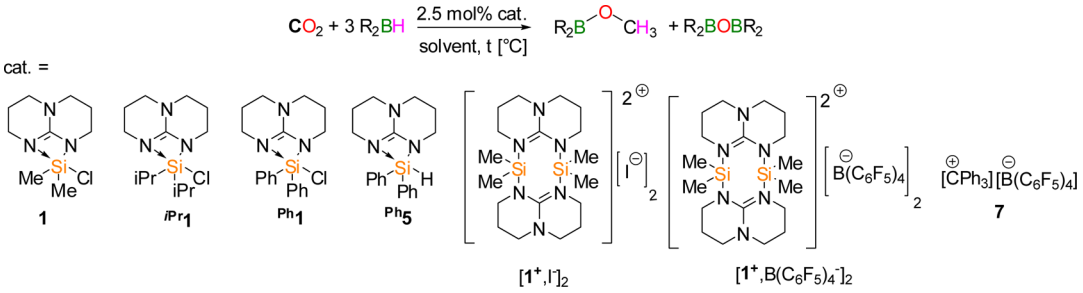

entry	catalyst	borane	T [°C]	t [h]	yield [%][b]	TOF (h^{-1})[c]
1	**1**	9-BBN	20	23(6.5)	100(77)	1.3 (3.7)
2[d]	**1**	9-BBN	20	78	17.5	0.1
3[e]	**1**	9-BBN	20	78	0	0.0
4[f]	**1**	9-BBN	20	78	83	0.3
5[g]	**1**	9-BBN	20	78	43	0.2
6	^{iPr}**1**	9-BBN	20	24	60	0.7
7	^{Ph}**1**	9-BBN	20	24	56	0.8
8	0.5[**1**$^+$,$B(C_6F_5)_4^-$]$_2$	9-BBN	20	72(3)	30(6)	0.1(0.9)
9	0.5[**1**$^+$,I^-]$_2$	9-BBN	20	24	100	1.3
10	**1**	catBH	70	120	74	0.5
11	^{iPr}**1**	catBH	70	67	31	0.3
12	^{Ph}**1**	catBH	70	96	44	0.3
13	0.5[**1**$^+$,$B(C_6F_5)_4^-$]$_2$	catBH	70	42	18	0.2
14	[**1**$^+$,I^-]$_2$	catBH	70	96	49	0.3
15	**1**	pinBH	90(70)	28(28)	75(21)	0.8(0.2)
16	^{iPr}**1**	pinBH	90(70)	16(28)	100(78)	2(0.8)
17	^{Ph}**1**	pinBH	90	28	82	0.9
18	0.5[**1**$^+$,$B(C_6F_5)_4^-$]$_2$	pinBH	90	90	50	0.6
19	0.5[**1**$^+$,I^-]$_2$	pinBH	90	96	40	0.5
20	^{Ph}**5**	catBH	70	96	40	0.3
21[h]	**7**	catBH	90	24	10	0.1

[a]Values in parentheses correspond to shorter reaction times with corresponding yields. [b]Reaction conditions: catalyst (2.5 mol %) in 400 μL of THF, (0.48 mmol of B−H) and 1 atm CO_2. Yields determined by ^{1}H NMR vs internal standard (mesitylene). [c]TOFs were calculated under steady-state regime as the derivative of TON (B−H bond used) vs reaction time. [d]In CH_3CN. [e]In pyridine. [f]In DCM. [g]In toluene. [h]In benzene.

h at 20 °C, MeOBBN was obtained in 60% yield using isopropyl compound ^{iPr}**1** (TOF = 0.7 h^{-1}) and in 56% yield with the phenyl analogue ^{Ph}**1** (TOF = 0.8 h^{-1}) (Table 1, entries 6 and 7). The nature of the anion X^- also has a drastic influence on the catalytic performances, and replacing the chloride ligand in **1** with the noncoordinating $B(C_6F_5)_4^-$ anion inhibits the catalytic hydroboration of CO_2 (entry 8, Table 1, TOFs up to 0.1 h^{-1}).[55] Poorly soluble in THF, [**1**$^+$,I^-]$_2$ promotes the reduction of CO_2 to MeOBBN, after an induction period of about 3 h, in 100% yield, after 24 h (TOF = 1.3 h^{-1} after induction period). [**1**$^+$,NTf_2^-]$_2$ does not react with CO_2 and shows no catalytic activity, in the presence of 9-BBN, presumably because of its very poor solubility in THF.

When 9-BBN is replaced with catechol borane (catBH), the selective reduction of CO_2 to methoxycatecholborane (MeOB-cat) proved less efficient requiring 120 h at 70 °C in 74% yield (TOF = 0.5 h^{-1}, entry 10, Table 1). Although the catalytic performances are modest, these results are interesting as neither the parent guanidine base TBD nor the dimeric boron analogue **III**, nor the N/B FLP-CO_2 adduct **V** (Scheme 2) show any catalytic activity with catBH and pinBH.[27] The same trends in reactivity are observed for catBH and 9-BBN when catalyst **1** is replaced with ^{iPr}**1**, ^{Ph}**1**, [**1**$^+$,I^-]$_2$, or [**1**$^+$,$B(C_6F_5)_4^-$]$_2$, and the catalytic activity plummets in the presence of poorly coordinating anions or with bulky silyl cations (entries 11−14 in Table 1). All together, these results suggest that the formation of a CO_2-adduct (e.g., **2**) facilitates the catalytic hydroboration of CO_2 with 9-BBN and catBH. Nevertheless, catalysts binding strongly to CO_2 such as [**1**$^+$,$B(C_6F_5)_4^-$]$_2$) are sluggish.

Although pinacolborane (pinBH) presents a much lower hydridic character and a weaker Lewis acidity at boron than 9-BBN or catBH,[56] it was found to be an efficient hydride source in the hydroboration of CO_2 with **1**. MeOBpin (75%) was obtained selectively after 28 h at 90 °C under 1 atm of CO_2, from pinBH and 2.5 mol % **1** (entry 15 in Table 1, TOF = 0.8 h^{-1}). Whereas metal-based catalysts have been shown to effectively catalyze the hydroboration of CO_2 using a variety of borane sources (e.g., $(9\text{-BBN})_2$, BH_3SMe_2, and catBH), few catalysts exist that utilize pinacolborane. For example, Sabo-Etienne and Bontemps et al. have reported a ruthenium hydride complex able to afford MeOBpin in a low 40% yield after 5 h at 70 °C (TOF = 5 h^{-1}).[52] Only three metal-free systems have been described so far as catalysts in the hydroboration of CO_2 with pinBH: Stephan et al. designed a ring expanded-carbene providing a mixture of two-, four-, and six-electron reduction products,[30] whereas Fontaine et al. prepared a phosphino-borane FLP producing 60% pinBOMe at 70 °C (TOF = 21 h^{-1}).[29,31] Recently, the group of Wegner reported a bidentate borane catalyst able to reduce CO_2 to the methanol level in

DOI: 10.1021/acscatal.6b00421
ACS Catal. 2016, 6, 4526−4535

Scheme 4. Computed Pathway for the Catalytic Hydroboration of CO_2 via CO_2 Activation (M05-2X/PCM THF)[a]

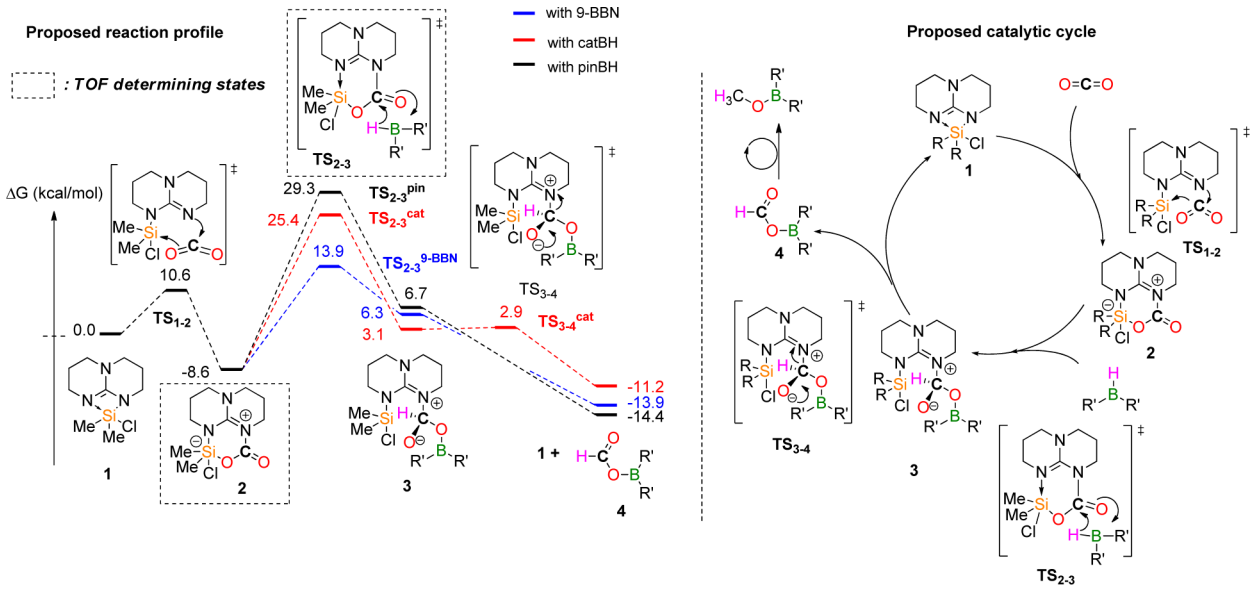

[a]Values given are the Gibbs Free Energies using **1** as a reference (G = 0.0 kcal/mol).

89% with pinBH at 70 °C with high reactivity (TOF = 93 h^{-1}).[33] As the catalyst itself possesses six active B−H bonds, this TOF-value must be considered with caution, and a TOF of around 16 h^{-1} is calculated per active B−H bond, facilitating its comparison with other catalysts bearing only one active site.

Strikingly, catalysts ^{iPr}**1** and ^{Ph}**1** perform better than **1** in the hydroboration of CO_2 with pinBH, while the opposite effect was noted with 9-BBN and catBH. MeOBpin is formed in 82 and 100% yield within 28 h at 90 °C with ^{Ph}**1** and ^{iPr}**1**, respectively, corresponding to TOFs of 0.9 and 2 h^{-1} (entries 16 an 17 in Table 1). Although the amino-borane catalyst of Fontaine and co-workers showed higher catalytic activity (TOF = 21 h^{-1}, at 70 °C),[31] ^{iPr}**1** is able to promote the formation of MeOBpin quantitatively without the formation of other reduction side products within only 16 h. In contrast to reactions with 9-BBN and catBH, the influence of the anion is less marked in the case of pinBH. Both compounds $[\mathbf{1}^+,B(C_6F_5)_4^-]_2$ and $[\mathbf{1}^+,I^-]_2$ exhibit a catalytic activity comparable to that of **1**, affording pinBOMe in 40 and 50% yield, respectively, after 24 h (TOFs of 0.5 and 0.6 h^{-1} respectively, Table 1, entries 18 and 19). It is remarkable that pinBH imposes different demands on the nature of the catalyst, and unlike 9-BBN and catBH, catalysts showing no CO_2 activation (e.g., ^{iPr}**1** and ^{Ph}**1**) are more efficient for the hydroboration of CO_2 with pinBH.

Reaction Mechanism and DFT Calculations. The catalytic hydroboration of CO_2 with **1**, $\mathbf{1}^+$, ^{iPr}**1**, and ^{Ph}**1** constitutes an appropriate system to explore the role and impact of FLP-CO_2 adducts in the reduction of CO_2 because these four active catalysts interact differently with CO_2. Whereas **1** and $\mathbf{1}^+$ form stable adducts with CO_2, replacing the methyl groups on the silicon atom in **1** with *i*-Pr or Ph substituents provides ^{iPr}**1** and ^{Ph}**1**, which do not react with CO_2. In addition, different behaviors and trends were noticed for 9-BBN and pinBH suggesting that different mechanisms might take place in this important transformation. Regardless of the nature of the hydroborane R_2BH, the formoxyborane $HCOOBR_2$ and the acetal $H_2C(OBR_2)_2$ are intermediates in the formation of $MeOBR_2$. In addition, the distribution of the products over time reveals that the reduction of CO_2 to methoxyborane is kinetically controlled by the first hydroboration step, yielding $HCOOBR_2$ (see SI page 6). The mechanism of the catalytic hydroboration of CO_2 to formoxyboranes has thus been investigated using both DFT calculations and stoichiometric reactions.

Mechanism Involving the Activation of CO_2. CO_2-adducts are often described as key-intermediates in the catalytic cycle of the CO_2 reduction processes,[25,57] and both adducts **IV** and **V** were shown to react with an electrophilic borane (9-BBN) to yield formate species.[27] In light of these data and the reaction chemistry of **1** described above, activation of CO_2 by **1** is a reasonable starting point for the hydroboration of CO_2 with **1** (Scheme 4). DFT calculations, performed at the M05-2X/PCM = THF/6-31+G* (6-311++G** for the active hydride) level of theory confirm that the formation of a CO_2 adduct $[\mathbf{2}^+,Cl^-]$ from **1** is indeed exergonic by −6.1 kcal/mol with a low activation barrier of only 10.6 kcal/mol (Scheme 4). Interestingly, the coordination of the chloride anion to the silylium center is also possible, and the corresponding CO_2 adduct **2** lies at −8.6 kcal/mol. These data are consistent with the experimental results showing a reversible CO_2 activation with **1** and the possible formation of hypervalent guanidinate chlorosilanes. Reduction of the activated CO_2 molecule in **2** with 9-BBN was found to involve the addition of the B−H bond to the unbound C═O functionality with a low lying transition state ($\mathbf{TS}_{2-3}$) at 13.9 kcal/mol. The resulting intermediate **3** features a tetrahedral carbon. Elimination of the product HCOOBBN (**4**) from **3** is essentially barrier-less and favored by the thermodynamics of the overall process (ΔG= −13.9 kcal/mol). The hydroboration of CO_2 with 9-BBN catalyzed by **1** thus involves three successive steps, namely, the activation of CO_2 by the intramolecular FLP, the addition of the hydroborane, and finally, the elimination of HCOOBBN to regenerate catalyst **1** (Scheme 4). Reduction of **3** before release by a second equivalent of hydride might therefore also be likely, although experimentally the first hydride transfer is rate determining (see SI). As depicted in Scheme 4, CO_2 adduct **2** and $\mathbf{TS}_{2-3}$ are the rate determining

DOI: 10.1021/acscatal.6b00421
ACS Catal. 2016, 6, 4526−4535

states, and they control the kinetics of the catalysis.[58−61] The computed energy span of 22.5 kcal/mol is much lower than the one required for the uncatalyzed addition of 9-BBN to CO_2 (30.8 kcal/mol)[27] and is consistent with a fast reaction at room temperature (computed TOF of 0.7 h^{-1}).[57] Notably, as the CO_2 adduct **2** constitutes a TOF determining intermediate (TDI), increasing its stability is detrimental to the catalytic performances. Computationally, removing the chloride anion in the energy surface depicted in Scheme 4, an energy span of 24.7 kcal/mol ($\mathbf{1}^+$ as 0.0 kcal/mol reference; see Figure S38) is obtained, that is, 2.2 kcal/mol higher than that with catalyst **1**. This result is in excellent agreement with the experimental findings pointing to a significant diminution of the catalytic performance when **1** is replaced with $[\mathbf{1}^+,B(C_6F_5)_4^-]_2$. Moreover, the addition of one equivalent of 9-BBN (monomer) to a 70:30 equilibrium mixture of $\mathbf{1}/[\mathbf{2}^+,Cl^-]$ results in the fast formation of the acetal $CH_2(OBBN)_2$ after only 2.5 h at RT, while a reaction time of 17 h is required for $[\mathbf{1}^+,B(C_6F_5)_4^-]_2$ (Scheme 5a,b). The formation of CO_2 adducts

Scheme 5. Stoichiometric and Catalytic Reactions between 1, $\mathbf{2}^+$, CO_2, and Hydroboranes

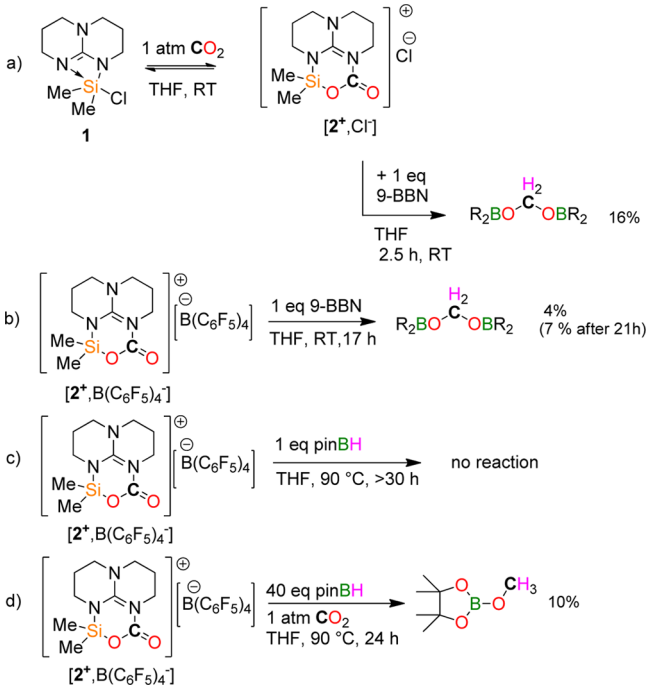

from $^{iPr}\mathbf{1}$ and $^{Ph}\mathbf{1}$ is around 4 kcal/mol higher in energy compared to that of **2** (see SI, Table S1). Although this destabilization could have a positive effect on the catalysis, it also results in a lower degree of activation of the CO_2 molecule and, hence, in a greater activation barrier of 25.2 and 22.6 kcal/mol for the rate determining C−H bond formation, for the *i*Pr and Ph substituted sytems, respectively (see SI, page 9 for detailed span values). Again, these results are in good qualitative agreement with the catalytic data showing a lower catalytic activity for $^{iPr}\mathbf{1}$ and $^{Ph}\mathbf{1}$ compared to that of **1**, and they emphasize the necessity for a fine balance in the activation of CO_2.

Obviously, changing 9-BBN with catBH or pinBH does not modify the energy level of the CO_2 adduct **2**. Nevertheless, it affects the position of the corresponding TS for the hydride transfer to CO_2 ($\mathbf{TS}_{2-3}$). Both catBH and pinBH possess a boron atom that is less Lewis acidic than 9-BBN because the π lone pairs on the oxygen substituents are delocalized into the boron vacant p orbital. As such, coordination of the hydroborane to the C═O group of the activated CO_2 molecule is disfavored, and the TOF determining $\mathbf{TS}_{2-3}^{cat}$ and $\mathbf{TS}_{2-3}^{pin}$ are higher in energy than **2** (spans of 34.0 and 37.9 kcal/mol for catBH and pinBH, respectively). The computed order of reactivity 9-BBN > catBH > pinBH is thus in agreement with the experimental observations. Nonetheless, a span of 39.7 kcal/mol is relatively high for a catalytic reaction proceeding at 70 °C, thereby questioning the validity of a mechanism relying on CO_2 activation for pinBH. In addition, while $^{iPr}\mathbf{1}$ presents a better catalytic performance than **1** with pinBH, its computed energy span is 1.8 kcal/mol higher in energy (37.9 kcal/mol). Experimentally, no reaction is observed upon mixing $[\mathbf{2}^+,B(C_6F_5)_4^-]_2$ with pinBH for >30 h at 90 °C, although 2.5 mol % $[\mathbf{1}^+,B(C_6F_5)_4^-]_2$ efficiently catalyzes the reduction of CO_2 to MeOBpin at 90 °C (Scheme 5 and Table 1, entry 18). These facts definitively rule out a mechanism relying on CO_2 activation for the hydroboration of CO_2 with pinBH, and an alternative pathway was sought.

Mechanism Involving the Electrophilic Activation of the Hydroborane. In order to account for the catalytic activity of **1** and $[\mathbf{1}^+,B(C_6F_5)_4^-]_2$ in the reduction of CO_2 with pinBH, an alternative mechanism was explored based on the potential electrophilic activation of the B−H bond with the catalyst (Scheme 6). Indeed, the ionization of the silicon-chloride bond is readily accessible in hypervalent chlorosilanes.[47] Starting from **1**, such dissociation would be also favored by the presence of an electrophile such as a hydroborane to yield masked silylium ion $\mathbf{1}^+$. The hydride transfer from R_2BHCl^- to $\mathbf{1}^+$ was computed for the three hydroborane reagents, to form hydrosilane **5** (Scheme 6). The formation of **5** and chloroborane R_2BCl (**6**) byproduct is slightly endergonic for the three hydroborane sources (+7.0 kcal/mol for 9-BBN, +10.9 kcal/mol for catBH, and +7.8 kcal/mol for pinBH, Scheme 6). Nevertheless, the respective transition state energies are all accessible, suggesting that it is a viable intermediate on the hypersurface (17.0 kcal/mol for 9-BBN, 21.8 kcal/mol for catBH, and 24.8 kcal/mol for pinBH, Scheme 6). Species **5** appears to be a potent reductant, and outersphere hydride transfer from the Si−H group in **5** to an incoming CO_2 molecule yields silylium $\mathbf{1}^+$ and the formate anion with a low energy barrier of 18.9 kcal/mol, in agreement with the reported reactivity of other hypervalent hydrosilanes toward CO_2.[62] Subsequent salt metathesis among $HCOO^-$, R_2BCl, and $\mathbf{1}^+$ finally regenerates catalyst **1** and releases formoxyborane $HCOOBR_2$, without any significant energy barrier (<6 kcal/mol).

$\mathbf{TS}_{5-4}$ associated with the reduction of CO_2 with **5** constitutes the highest energy rate determining state in this pathway.[63] Interestingly, the structure of $\mathbf{TS}_{5-4}$ does not depend on the nature of the hydroborane, although its energy level is indirectly dictated by the formation of the chloroborane coproduct R_2BCl (**6**). Although catalyst **1** is the lowest energy state in this pathway, CO_2 adduct **2** easily forms under the applied conditions, as revealed by ^1H NMR spectroscopy, and it should therefore be included on the energy surface. **2** is thus an off-cycle intermediate that further enlarges the surface landscape yielding energetic spans of 34.5 kcal/mol (9-BBN), 35.3 kcal/mol (pinBH), and 38.3 kcal/mol (catBH) for the different hydroboranes.

DOI: 10.1021/acscatal.6b00421
ACS Catal. 2016, 6, 4526−4535

Scheme 6. Computed Pathway for the Electrophilic Activation of Hydroboranes in the Reduction of CO_2 to Formoxyboranes (M05-2X/PCM THF)[a]

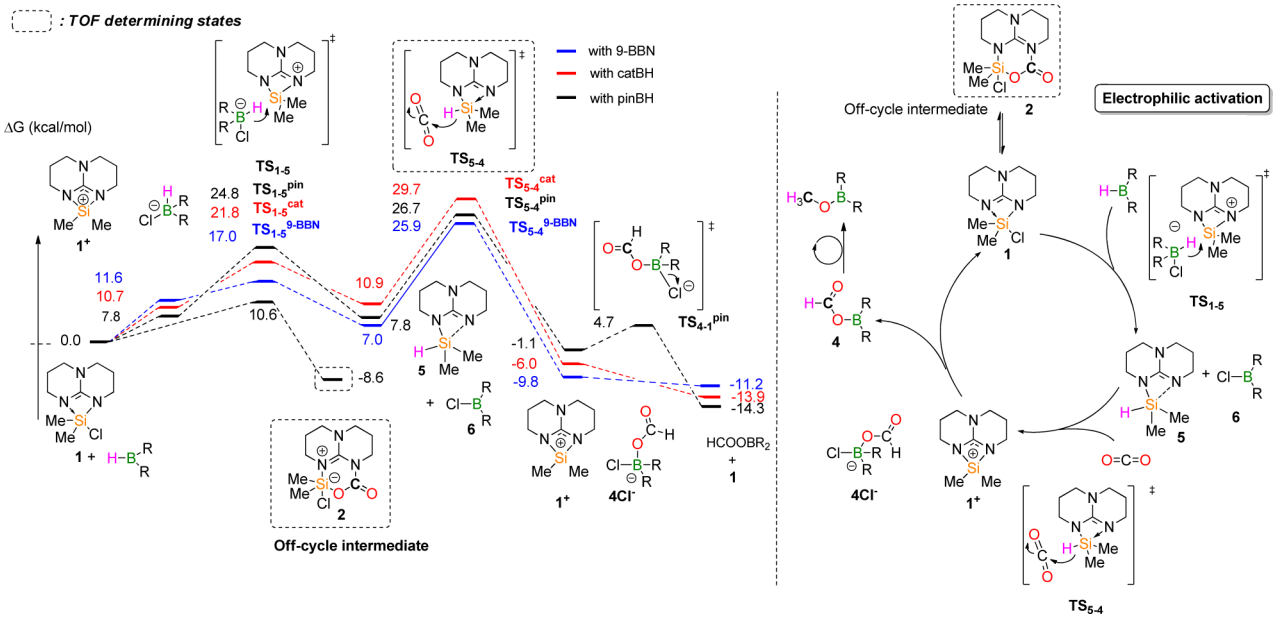

[a]Values given are Gibbs Free Energies with respect to **1** (0.0).

This mechanistic route hence highlights two important experimental observations. First, an electrophilic pathway significantly lowers the energetic span (35.3 kcal/mol) by about 3 kcal/mol for the hydroboration of CO_2 with pinBH compared to a route where CO_2 is activated via the formation of an adduct (37.9 kcal/mol). Second, a stable CO_2-adduct hampers reaction kinetics in CO_2 hydroboration under electrophilic activation, as witnessed by the lower reactivity of $[\mathbf{1}^+,B(C_6F_5)_4^-]_2$ compared to that of **1**. In fact, such a mechanism also explains the differences in reactivity among **1**, ^{iPr}**1**, and ^{Ph}**1**, but care has to be taken to avoid quantitative conclusions, as the calculated spans are close in energy. Computationally, the energy span for the catalytic hydroboration of CO_2 with pinBH decreases from 35.3 kcal/mol with **1** to 34.2 and 32.4 kcal/mol with ^{Ph}**1** and ^{iPr}**1**, respectively. The DFT model is thus consistent with the experimental data providing the following order of reactivity: ^{iPr}**1** > ^{Ph}**1** > **1**. Although the order of reactivity is reproduced correctly, these results have to be taken as a qualitative measure, given the accuracy of the DFT models. It is notable that, although the TOF-limiting transition state with ^{iPr}**1** corresponds to the hydride abstraction from pinBH ($\mathbf{TS}_{5-4}$), the main factor governing its higher catalytic activity is the destabilization of CO_2-adduct ^{iPr}**2** (+3.7 kcal/mol with respect to **2**) (see SI, Table S1).

To further emphasize the feasibility of CO_2 reduction by a base-substituted silane **5** (Scheme 7), the synthesis of such a species was attempted. Guanidine substituted hydrosilane ^{Ph}**5** is easily accessible through dehydrogenative coupling of TBD with diphenylsilane and shows a characteristic hydride peak at 5.03 ppm in the ^{1}H NMR (Scheme 7 and Figure S28). Crystals suitable for X-ray analysis were obtained by slowly cooling down a concentrated acetonitrile solution of ^{Ph}**5** from 90 °C to room temperature (Figure 3). With bond angles of 97.4, 114.7(2)° and 116.8(2) for N1−Si−H1, N1−Si−C8a, and N1−Si−C14a, respectively, the silicon geometry is slightly distorted from a tetrahedron, although a ω-bond as in **1** or ^{iPr}**1** is less likely due to a small bond angle of 153.6° for N2−Si−H1 and a long N2−Si distance of 2.648(5) Å. Under 1 atm of CO_2, a THF solution of ^{Ph}**5** evolves within minutes at room

Scheme 7. Reduction of CO_2 with ^{Ph}5 to a Formate Species

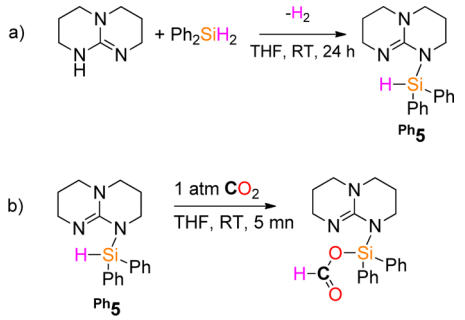

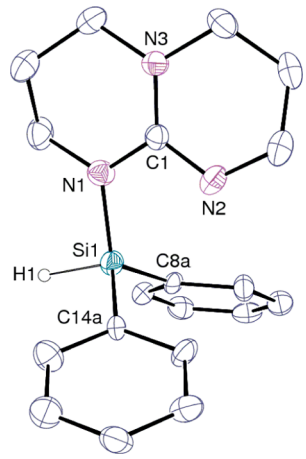

Figure 3. ORTEP view of ^{Ph}**5**. Only one position of the disordered groups is represented (see SI for details). Selected bond lengths (Å): Si1−N1 1.722(3), Si1−H1 1.427, N1−C1 1.341(4), and N2−C1 1.323(4).

DOI: 10.1021/acscatal.6b00421
ACS Catal. 2016, 6, 4526−4535

temperature to yield a formate species (Scheme 7 and Figure S30). In the absence of an electrophilic scavenger, such as a chloroborane, this species then converts to formylated TBD by deoxygenation of the formate anion (Figure S30). This chemical behavior demonstrates the strong reductive capability of ^{Ph}**5** in the presence of CO_2,[64] in agreement with the DFT model depicted in Scheme 6.

The catalytic implication of ^{Ph}**5** was further assessed in the reduction of CO_2 with catBH. ^{Ph}**5** shows comparable activity as the related phenyl catalyst ^{Ph}**1** (TOF = 0.3 h^{-1} in both cases) providing CH_3OBcat in 40% yield after 96 h at 70 °C (44% for ^{Ph}**1**, Table 1, entries 20 and 12).

Overall, the mechanistic route depicted in Scheme 6 relies on the abstraction of a hydride from the hydroborane reagent with the Lewis acid catalyst and its subsequent transfer to CO_2 for the reduction of a C═O bond. This route is hence reminiscent of the work of Piers and Gevorgyan groups on the hydrosilylation of C═O and C−O bonds, where the electrophilic borane ($B(C_6F_5)_3$) abstracts the hydride from the hydrosilane.[64−70] Here, DFT calculations suggest that the inverse reaction should also be possible. With the work of Oestreich and co-workers[71,72] on the transient formation of such Si−H−B species during the hydrosilylation of carbonyl functional groups and the recent isolation and characterization of such a species by Piers and co-workers,[73] the availability of a transition state ($\mathbf{TS}_{1-5}$) for the hydride transfer from a chloroborate (e.g., $[pinBH-Cl]^-$) to the masked silylium $\mathbf{1}^+$ is further accredited. Interestingly, such a mechanism relying on an electrophilic activation of a hydroborane reductant is unprecedented in hydroboration chemistry, although it resembles the mode of action of Lewis acid catalysts in hydrosilylation chemistry. It is found to be favored for electron rich boranes such as pinBH (and possibly catBH, although DFT calculation does not allow us to draw a final conclusion), with a boron center stabilized by electron donors.

Altogether, these results provide a clearer perspective of the role of FLP-CO_2 adducts in the catalytic reduction of CO_2 and of the different mechanisms at play in the organocatalytic hydroboration of CO_2. Organic catalysts have been shown to promote the hydroboration of CO_2 via three different modes (Scheme 8). First, strong nucleophiles favor the hydride transfer to CO_2 by increasing the hydridicity of the B−H linkage by coordination to the boron center (Scheme 8A). As an example, catalyst Me-TBD or pro-azaphosphatranes operate through this process.[27,74] In a recent study by Bourissou and Fontaine,[32] the importance of an intermediate formaldehyde adduct was highlighted, which can also serve as a Lewis base. In contrast, Lewis acids may abstract the hydride of the B−H bond to yield a boron electrophile and convert the catalyst to a strong hydride donor, as observed for ^{iPr}**1** with pinBH (Scheme 8B). In these two mechanisms, the formation of stable CO_2 adducts hampers the catalysis by stabilizing the catalyst's resting state. Finally, the organocatalyst can also activate the CO_2 molecule, directly. As CO_2 is a weak Lewis base, this mode of action usually involves a bifunctional activation of CO_2 with the cooperative effect of a Lewis base and a Lewis acid (Scheme 8C). Catalysts **1**, $\mathbf{2}^+$, and **IV** were shown to follow this path, with 9-BBN. Importantly, the degree of activation of the CO_2 molecule must be finely tuned to open this reduction path. Indeed, the "*activation*" of CO_2 in the form of an adduct is both deleterious and necessary to the catalytic activity, as it stabilizes the lowest intermediate in the potential energy surface yet prepares CO_2 for the subsequent reduction step by removing electron density from the carbon by coordination to the Lewis acid. It is noteworthy that future catalytic systems based on this approach should thus target compounds that show a low affinity for CO_2, based on thermodynamics, yet increase the electrophilicity of the carbon center with strong Lewis acids.

Scheme 8. Different Modes of Action of an Organocatalyst in the Hydroboration of CO_2

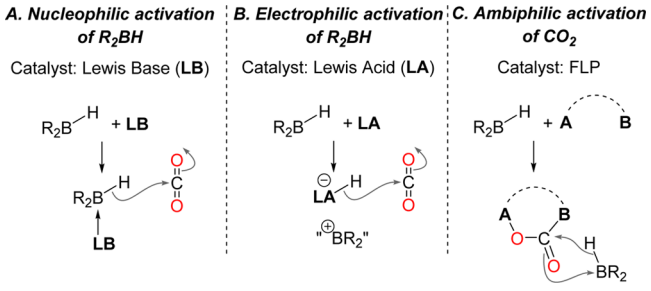

CONCLUSIONS

A novel class of intramolecular nitrogen−silylium FLPs, e.g., $TBDSiR_2Cl$ (R = Me, ^{i}Pr, and Ph) and their cationic derivatives have been reported, and their reactivity with CO_2 has been investigated. Formation and stability of the CO_2-adducts can be modulated with the steric and electronic environment at the silicon center, and only the methylated CO_2−FLP have been observed and characterized. All of these novel silicon species were shown to promote the catalytic hydroboration of CO_2 to the methoxide level, in high yield under mild reaction conditions. DFT calculations were carried out, in support of experimental results, to better explore the role of FLP-CO_2 adducts in the catalytic reduction of CO_2 with 3 different boranes (9-BBN, catBH, and pinBH). To date, CO_2-adducts $\mathbf{2}^+$ and **V**, where CO_2 is activated by a N/Si^+ or N/B intramolecular FLP, remain the only two examples of stable FLP-CO_2 adducts exhibiting a catalytic activity in the hydroelementation of CO_2.

From a mechanistic point of view, the reduction of CO_2 by 9-BBN with **1** relies on a hydride transfer from boron to carbon through a [2 + 2] mechanism, where the B−H bond adds to the C═O bond of the activated CO_2 molecule in the FLP-CO_2 adduct. However, using pinBH with ^{iPr}**1** as catalyst a novel electrophilic pathway is at play. For catBH and other catalysts, a clear distinction between both pathways cannot be made. Nevertheless, a strong stabilization of CO_2 in the form of an adduct is deleterious to the catalytic activity in all cases.

ASSOCIATED CONTENT

Supporting Information

The Supporting Information is available free of charge on the ACS Publications website at DOI: 10.1021/acscatal.6b00421.

Experimental procedures, characterization of compounds, kinetic profile of catalytic CO_2 hydroboration, crystallographic data, Cartesian coordinates of all optimized stationary points and transition states with the corresponding energies and lowest frequencies, and overview of the energetic spans of the different proposed reaction mechanisms including different catalysts and hydroboranes sources, as well as an alternative reaction pathway (PDF)

DOI: 10.1021/acscatal.6b00421
ACS Catal. 2016, 6, 4526−4535

X-ray data (CIF)

AUTHOR INFORMATION

Corresponding Author

*Fax: +33-1-6908-6640. E-mail: thibault.cantat@cea.fr.

Notes

The authors declare no competing financial interest.

ACKNOWLEDGMENTS

For financial support of this work, we acknowledge CEA, CNRS, the University Paris-Saclay, the CHARMMMAT Laboratory of Excellence, and the European Research Council (ERC Starting Grant Agreement no. 336467). T.C. thanks the Fondation Louis D. − Institut de France for its great support. N.v.W. thanks S. Kozuch for providing the Autotof software.

REFERENCES

(1) Fiorani, G.; Guo, W.; Kleij, A. W. *Green Chem.* **2015**, *17*, 1375−1389.
(2) Aresta, M.; Nobile, C. F.; Albano, V. G.; Forni, E.; Manassero, M. *J. Chem. Soc., Chem. Commun.* **1975**, *0*, 636−637.
(3) Tlili, A.; Blondiaux, E.; Frogneux, X.; Cantat, T. *Green Chem.* **2015**, *17*, 157−168.
(4) Leitner, W. *Coord. Chem. Rev.* **1996**, *153*, 257−284.
(5) Walther, D. *Nachr. Chem., Tech. Lab.* **1992**, *40*, 1214−1227.
(6) Walther, D.; Ruben, M.; Rau, S. *Coord. Chem. Rev.* **1999**, *182*, 67−100.
(7) Fernandez-Alvarez, F. J.; Aitani, A. M.; Oro, L. A. *Catal. Sci. Technol.* **2014**, *4*, 611−624.
(8) Vaska, L. *J. Mol. Catal.* **1988**, *47*, 381−388.
(9) Gibson, D. H. *Coord. Chem. Rev.* **1999**, *185−186*, 335−355.
(10) Gibson, D. H. *Chem. Rev.* **1996**, *96*, 2063−2096.
(11) Weyers, G.; Steimann, M.; Kuhn, N. *Z. Naturforsch.* **1999**, *54b*, 427.
(12) Villiers, C.; Dognon, J.-P.; Pollet, R.; Thuéry, P.; Ephritikhine, M. *Angew. Chem., Int. Ed.* **2010**, *49*, 3465−3468.
(13) Murphy, L. J.; Robertson, K. N.; Kemp, R. A.; Tuononen, H. M.; Clyburne, J. A. C. *Chem. Commun.* **2015**, *51*, 3942−3956.
(14) Stephan, D. W. *Dalton Transactions* **2009**, 3129−3136.
(15) Stephan, D. W. *Org. Biomol. Chem.* **2008**, *6*, 1535−1539.
(16) Erker, G. *C. R. Chim.* **2011**, *14*, 831−841.
(17) Stephan, D. W. *Acc. Chem. Res.* **2015**, *48*, 306−316.
(18) Fontaine, F.-G.; Courtemanche, M.-A.; Légaré, M.-A. *Chem. - Eur. J.* **2014**, *20*, 2990−2996.
(19) Mömming, C. M.; Otten, E.; Kehr, G.; Fröhlich, R.; Grimme, S.; Stephan, D. W.; Erker, G. *Angew. Chem., Int. Ed.* **2009**, *48*, 6643−6646.
(20) Theuergarten, E.; Bannenberg, T.; Walter, M. D.; Holschumacher, D.; Freytag, M.; Daniliuc, C. G.; Jones, P. G.; Tamm, M. *Dalton Transactions* **2014**, *43*, 1651−1662.
(21) Stephan, D. W. *J. Am. Chem. Soc.* **2015**, *137*, 10018−10032.
(22) Ménard, G.; Gilbert, T. M.; Hatnean, J. A.; Kraft, A.; Krossing, I.; Stephan, D. W. *Organometallics* **2013**, *32*, 4416−4422.
(23) Travis, A. L.; Binding, S. C.; Zaher, H.; Arnold, T. A. Q.; Buffet, J.-C.; O'Hare, D. *Dalton Transactions* **2013**, *42*, 2431−2437.
(24) Appelt, C.; Westenberg, H.; Bertini, F.; Ehlers, A. W.; Slootweg, J. C.; Lammertsma, K.; Uhl, W. *Angew. Chem., Int. Ed.* **2011**, *50*, 3925−3928.
(25) Ménard, G.; Stephan, D. W. *J. Am. Chem. Soc.* **2010**, *132*, 1796−1797.
(26) Bertini, F.; Lyaskovskyy, V.; Timmer, B. J. J.; de Kanter, F. J. J.; Lutz, M.; Ehlers, A. W.; Slootweg, J. C.; Lammertsma, K. *J. Am. Chem. Soc.* **2012**, *134*, 201−204.
(27) Das Neves Gomes, C.; Blondiaux, E.; Thuéry, P.; Cantat, T. *Chem. - Eur. J.* **2014**, *20*, 7098−7106.
(28) Barnett, B. R.; Moore, C. E.; Rheingold, A. L.; Figueroa, J. S. *Chem. Commun.* **2015**, *51*, 541−544.
(29) Courtemanche, M.-A.; Légaré, M.-A.; Maron, L.; Fontaine, F.-G. *J. Am. Chem. Soc.* **2014**, *136*, 10708−10717.
(30) Wang, T.; Stephan, D. W. *Chem. - Eur. J.* **2014**, *20*, 3036−3039.
(31) Courtemanche, M.-A.; Légaré, M.-A.; Maron, L.; Fontaine, F.-G. *J. Am. Chem. Soc.* **2013**, *135*, 9326−9329.
(32) Declercq, R.; Bouhadir, G.; Bourissou, D.; Légaré, M.-A.; Courtemanche, M.-A.; Nahi, K. S.; Bouchard, N.; Fontaine, F.-G.; Maron, L. *ACS Catal.* **2015**, *5*, 2513−2520.
(33) Lu, Z.; Hausmann, H.; Becker, S.; Wegner, H. A. *J. Am. Chem. Soc.* **2015**, *137*, 5332−5335.
(34) Berkefeld, A.; Piers, W. E.; Parvez, M. *J. Am. Chem. Soc.* **2010**, *132*, 10660−10661.
(35) Cantat, T.; Gomes, C.; Blondiaux, E.; Jacquet, O. Method for preparing oxyborane compounds. C07F 5/02 (2006.01), C07B 59/00 (2006.01), G01N 33/60 (2006.01). WO/2014/162266, 2014.
(36) Reißmann, M.; Schäfer, A.; Jung, S.; Müller, T. *Organometallics* **2013**, *32*, 6736−6744.
(37) Schäfer, A.; Reißmann, M.; Schäfer, A.; Saak, W.; Haase, D.; Müller, T. *Angew. Chem., Int. Ed.* **2011**, *50*, 12636−12638.
(38) Weicker, S. A.; Stephan, D. W. *Chem. - Eur. J.* **2015**, *21*, 13027−13034.
(39) Herrington, T. J.; Ward, B. J.; Doyle, L. R.; McDermott, J.; White, A. J. P.; Hunt, P. A.; Ashley, A. E. *Chem. Commun.* **2014**, *50*, 12753−12756.
(40) Douvris, C.; Ozerov, O. V. *Science* **2008**, *321*, 1188−1190.
(41) Lambert, J. B.; Zhang, S.; Stern, C. L.; Huffman, J. C. *Science* **1993**, *260*, 1917−1918.
(42) Reed, C. A. *Acc. Chem. Res.* **1998**, *31*, 325−332.
(43) Maaranen, J.; Andell, O. S.; Vanne, T.; Mutikainen, I. *J. Organomet. Chem.* **2006**, *691*, 240−246.
(44) Andell and co-workers solved a dimeric structure of **1** by cooling down a refluxing pentane solution to −30 °C. This might indicate a higher thermodynamic stability of the dimeric structure.
(45) Pounds, A. J. *J. Chem. Educ.* **2007**, *84*, 43.
(46) Weinhold, F.; Landis, C. R. *Valency and Bonding: A Natural Bond Orbital Donor-Acceptor Perspective*; Cambridge University Press: Cambridge, U.K., 2005.
(47) Kummer, D.; Abdel Halim, S. H.; Kuhs, W.; Mattern, G. *J. Organomet. Chem.* **1993**, *446*, 51−65.
(48) Crystals suitable for X-ray analysis were obtained by slow diffusion of pentane into a concentrated solution of $[\mathbf{1}^+,I^-]_2$ in DMF. However, the solved structure shows the decomposition of $[\mathbf{1}^+,I^-]_2$ in DMF with complete deoxygenation of several DMF molecules and four TBD residues, as well as four iodides in the unit cell.
(49) Chakraborty, S.; Zhang, J.; Krause, J. A.; Guan, H. *J. Am. Chem. Soc.* **2010**, *132*, 8872−8873.
(50) Huang, F.; Zhang, C.; Jiang, J.; Wang, Z.-X.; Guan, H. *Inorg. Chem.* **2011**, *50*, 3816−3825.
(51) Shintani, R.; Nozaki, K. *Organometallics* **2013**, *32*, 2459−2462.
(52) Bontemps, S.; Vendier, L.; Sabo-Etienne, S. *Angew. Chem., Int. Ed.* **2012**, *51*, 1671−1674.
(53) Sgro, M. J.; Stephan, D. W. *Angew. Chem., Int. Ed.* **2012**, *51*, 11343−11345.
(54) We chose to calculate the TOF following the proposition of Kozuch and Martin (see ref 62), i.e., as the derivative of the number of turnovers (number of B−H bonds used) per catalyst with respect to the reaction time under a steady state regime.
(55) $[\mathbf{1}^+,NTf_2^-]_2$ is almost insoluble in THF and showed no catalytic activity under the employed reaction conditions.
(56) Plumley, J. A.; Evanseck, J. D. *J. Phys. Chem. A* **2009**, *113*, 5985−5992.
(57) Lu, Z.; Wang, Y.; Liu, J.; Lin, Y.-j.; Li, Z. H.; Wang, H. *Organometallics* **2013**, *32*, 6753−6758.
(58) Kozuch, S.; Shaik, S. *Acc. Chem. Res.* **2011**, *44*, 101−110.
(59) Uhe, A.; Kozuch, S.; Shaik, S. *J. Comput. Chem.* **2011**, *32*, 978−985.
(60) Stephan, D. W.; Erker, G. *Chemical Science* **2014**, *5*, 2625−2641.
(61) Kozuch, S. *Wiley Interdiscip. Rev. Comput. Mol. Sci.* **2012**, *2*, 795−815.

DOI: 10.1021/acscatal.6b00421
ACS Catal. 2016, 6, 4526−4535

(62) Kozuch, S.; Martin, J. M. L. *ACS Catal.* **2012**, *2*, 2787−2794.
(63) The formation of hypervalent hydrosilanes has also been proposed as a competent catalytic pathway in the hydrosilylation of CO_2, based on DFT calculation. See: Zhou, Q.; Li, Y. *J. Am. Chem. Soc.* **2015**, *137*, 10182−10189.
(64) Arya, P.; Boyer, J.; Corriu, R. J. P.; Lanneau, G. F.; Perrot, M. *J. Organomet. Chem.* **1988**, *346*, C11−C14.
(65) Gevorgyan, V.; Liu, J.-X.; Rubin, M.; Benson, S.; Yamamoto, Y. *Tetrahedron Lett.* **1999**, *40*, 8919−8922.
(66) Gevorgyan, V.; Rubin, M.; Benson, S.; Liu, J.-X.; Yamamoto, Y. *J. Org. Chem.* **2000**, *65*, 6179−6186.
(67) Gevorgyan, V.; Rubin, M.; Liu, J.-X.; Yamamoto, Y. *J. Org. Chem.* **2001**, *66*, 1672−1675.
(68) Blackwell, J. M.; Foster, K. L.; Beck, V. H.; Piers, W. E. *J. Org. Chem.* **1999**, *64*, 4887−4892.
(69) Blackwell, J. M.; Sonmor, E. R.; Scoccitti, T.; Piers, W. E. *Org. Lett.* **2000**, *2*, 3921−3923.
(70) Parks, D. J.; Blackwell, J. M.; Piers, W. E. *J. Org. Chem.* **2000**, *65*, 3090−3098.
(71) Hog, D. T.; Oestreich, M. *Eur. J. Org. Chem.* **2009**, *2009*, 5047−5056.
(72) Rendler, S.; Oestreich, M. *Angew. Chem., Int. Ed.* **2008**, *47*, 5997−6000.
(73) Houghton, A. Y.; Hurmalainen, J.; Mansikkamäki, A.; Piers, W. E.; Tuononen, H. M. *Nat. Chem.* **2014**, *6*, 983−988.
(74) Blondiaux, E.; Pouessel, J.; Cantat, T. *Angew. Chem., Int. Ed.* **2014**, *53*, 12186−12190.

DOI: 10.1021/acscatal.6b00421
ACS Catal. 2016, 6, 4526−4535